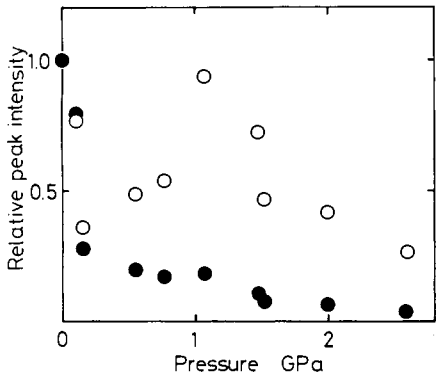

Figure 7. Pressure dependence of the relative peak intensities of fluorescence (●) and phosphorescence (○) of the Pt_2 crystals. The intensities are normalized to the values at atmospheric pressure.

manifested by the absence of T-T annihilation.[21,22]

Emission Intensity of the Pt_2 Crystal. Since it is difficult to separate these three emissions from each other, the peak intensities of each emission is taken to represent the relative quantum efficiency. As the full width at half-maximum is also dependent on pressure, this is not an ideal procedure and should be considered as a qualitative index. The relative value of the intensity at ambient pressure to that at atmospheric pressure was chosen for the following analysis.

The pressure dependence of the relative emission intensity is shown in Figure 7 for fluorescence (I_F) and phosphorescence (I_P). I_F decreased very much with pressure up to 0.2 GPa, whereas it is almost constant over 0.2 GPa. I_P decreases rapidly up to 0.2 GPa, increases (0.2-1.0 GPa), and decrease again at high pressure.

The initial decrease in I_F and I_P up to about 0.2 GPa is possibly ascribed to an increase of nonradiative decay from the S_1 state to the S_0 state. Application of pressure increases both intra- and intermolecular interaction so that the nonradiative pathway is facilitated. Ultimately, the pressure effect appears as the S_1 state excimer formation, which is reminiscent of strong inter Pt-Pt interaction, as discussed above. I_P increases between 0.2 and 1 GPa, reaching a maximum value comparable to the value at atmospheric pressure, while I_F stays nearly constant or decrease slightly in this pressure region. If an increase in the intersystem crossing efficiency were the origin of the increase in I_P, I_F should have decreased more drastically to compensate for the increase in I_P. The observed decrease in I_F is much smaller than expected. The reason is consequently attributed to an enhanced phosphorescence rate constant (k_P). Since T-T annihilation participates in the crystals, the estimation of k_P requires complex mathematical analysis.[21,22] The change in k_P is however very likely as judged by pressure-induced change in absorption spectrum. The absorption energy maximum and the molar extinction coefficient (ϵ) of Pt_2 in aqueous solution are 452 nm (110 M^{-1} cm^{-1}; $^1A_{1g} \rightarrow {}^3A_{2u}$) and 367 nm (33 200 M^{-1} cm^{-1}; $^1A_{1g} \rightarrow {}^1A_{2u}$). In the crystal at atmospheric pressure, the absorption at 367 nm is mainly observed, since ϵ(452) is very small. Under high pressure, the metal-metal interaction become stronger, so that the S-T mixing and hence ϵ(452) are expected to be enhanced.[23] This enhanced S-T mixing brings about an increase in k_P and thus I_P. Further increase in applied pressure (above 1 GPa) causes stronger intermolecular interaction, and the intermolecular processes such as T-T annihilation and other bimolecular nonradiative decay paths become dominant. As a consequence, the drop of I_P is observed above 1 GPa.

The lower energy shifts of both fluorescence and phosphorescence with increasing pressure are the manifestations that an increasing in the d-d splitting is caused by reduction of the intra Pt-Pt distance. The pressure-dependent new emission is most likely to be excimer emission, which is observable only in the crystal. Application of high pressure changes both intermolecular and intramolecular interaction and thus influences emission properties as well as their dynamic photophysical process.[22]

Acknowledgment. We express our hearty thanks to Prof. T. Azumi of Tohoku University for his enlightening discussion. Our thanks are also due to Dr. S. Ochiai of JEOL for collaboration in IR spectroscopy.

(21) Tanaka, Y.; Azumi, T. *Inorg. Chem.* **1986**, *25*, 248; *Chem. Phys. Lett.* **1986**, *132*, 357.

(22) Uchida, T.; Kim, H.-B.; Hiraga, T.; Tazuke, S. *J. Am. Chem. Soc.*, submitted.

(23) Considerable S-T mixing is expected for complexes of heavy metals since spin-orbit coupling is large, which is further enhanced under high pressure. In fact, our preliminary absorption spectroscopy by using the DAC indicated that ϵ(452) of $K_4[Pt_2(P_2O_5H_2)_4]$ crystals increased under high pressure.[1b] However, a recent report by Stroud et al. did not mention the enhancement of S-T mixing for $(n\text{-}Bu_4N)_4[Pt_2(P_2O_5H_2)_4]$ crystals.[11] The difference in the countercation is an important factor affecting the density of crystals mainly owing to the difference in size.[22] This discrepancy between Stroud's and our result may therefore be attributed to the difference in the countercation.

Pressure Effects on the Absorption and Emission of Tetracyanoplatinates(II) in Solution

A. Lechner and G. Gliemann*

Contribution from the Institut für Physikalische und Theoretische Chemie, Universität Regensburg, D-8400 Regensburg, Federal Republic of Germany. *Received February 13, 1989*

Abstract: Absorption and emission spectra of solutions of different tetracyanoplatinate(II) compounds as functions of concentration, solvent, temperature (278 K $\lesssim T \lesssim$ 333 K), and applied pressure (1 bar $\leq p \leq$ 17 kbar) are reported. The spectra of aqueous solutions with $c_0 \gtrsim 0.1$ M at room temperature and $p = 1$ bar exhibit features that can be assigned to the formation of oligomers $[Pt(CN)_4]_n^{2n-}$ with $n \geq 3$. Increasing the pressure lowers the minimum concentration at which oligomers are formed, shifts the equilibrium to oligomers of larger size, and reduces the intercomplex distance in the oligomers.

The optical properties of tetracyanoplatinates(II) (≡CP) are changed considerably, if the compounds are transferred from their dilute aqueous solutions to the crystalline state. The reason for this is a strong coupling between neighboring complex ions in the single crystals, which contain mutually parallel columns of closely stacked $[Pt(CN)_4]^{2-}$ ions.[1] This structural feature of the crystals

0002-7863/89/1511-7469$01.50/0

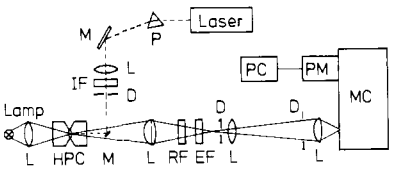

Figure 1. Spectrometer for the measurement of absorption and emission spectra of solutions at different pressures. D, diaphragm; EF, edge filter; HPC, high-pressure cell; IF, interference filter; L, quartz glass lens; M, mirror; MC, monochromator; P, quartz glass prism; PC, personal computer; PM, photomultiplier; RF, reflection filter.

entails a distinct anisotropy of their optical absorption and emission, which can be influenced drastically by variations of temperature[2-4] and by application of magnetic fields[5,6] and high pressures.[7,8]

Whereas dilute aqueous solutions of tetracyanoplatinates(II) show no emission, for concentrated solutions of BaCP, MgCP, and K_2CP, a bright emission has been reported by Khvostikov,[9] Ryskin and Tolstoi et al.,[10] Rossiello and Furlani,[11] Webb and Rossiello,[12] and more recently Schindler et al.[13] The latter authors have studied the concentration dependence of the room-temperature absorption and emission of aqueous solutions of K_2CP and BaCP. For concentrated solutions, the absorption and the emission spectra have been found to be distinctly different both from the single-crystal spectra and from the spectra of the dilute solutions. Schindler et al.[13] have discussed the matter of possible oligomer formation in solution, and they have assigned several features of the spectra to oligomers $[Pt(CN)_4]_n^{2n-}$ of different size ($n \geq 3$).

The purpose of our paper is to obtain additional information on the nature of the oligomers, e.g., on the conditions of their formation and the type of intercomplex coupling in the oligomers. To this end, the absorption and emission spectra of differently concentrated solutions of tetracyanoplatinate(II) compounds have been measured as functions of temperature (278 K $\lesssim T \lesssim$ 333 K) and applied pressure (1 bar $\leq p \lesssim$ 17 kbar). From the application of high pressure, a distinct influence both on the stacking of the complex ions to oligomers and on the intercomplex coupling in the oligomers is expected.

Experimental Section

The compounds $M_x[Pt(CN)_4]$ with $M_x = K_2$, Ba, Sr, and Cs_2 have been prepared according to the procedures in ref 14 and 15, respectively. For the preparation of $((n\text{-}C_4H_9)_4N)_2[Pt(CN)_4]$, a method described in ref 16 has been used. The concentration values c_0 of the solutions are based on the Pt(II) formality at p = 1 bar.

The optical absorption and emission spectra of solutions at high pressure have been measured by the spectrometer shown in Figure 1.

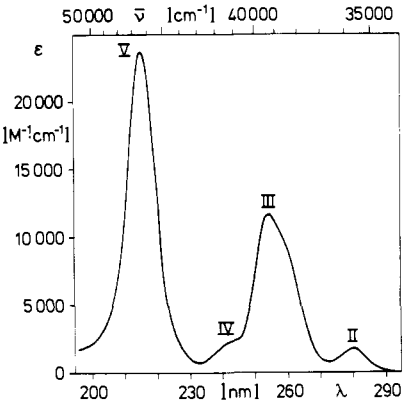

Figure 2. Absorption spectrum of a dilute aqueous solution of BaCP. $c_0 \sim 10^{-4}$ M. T = 298 K. p = 1 bar.

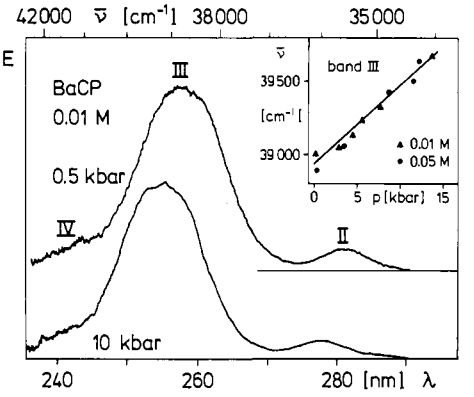

Figure 3. Absorption bands II–IV of an aqueous solution of BaCP at p = 1 bar and 10 kbar. c_0 = 0.01 M. T = 298 K. Inset: $\bar{\nu}$ of the maximum of absorption band III as a function of pressure, p, with c_0 = 0.01 and 0.05 M. T = 298 K.

The solutions were filled into the hole (diameter ~ 0.4 mm) of the gasket of a modified sapphire cell of Bridgman's opposed anvil type.[17] As gasket material, "Inconel" has been proved to be an efficient sealant for aqueous solutions. The pressure within the cell was determined by the pressure shift of the R lines of small ruby crystals added to the liquid sample.[18] To avoid an interference of the ruby calibration with the luminescence of chromium(III) centers in the sapphires, anvils with very weak chromium(III) luminescence were selected. For pressure calibration, (i) the exciting beam was focused on a ruby crystal and (ii) the emitting ruby crystal was imaged on a (variable) diaphragm, which suppresses the sapphire luminescence. For absorption spectroscopy, a deuterium lamp (60 W) was used as the radiation source, whereas the emission was excited by an argon ion laser. Because of the intensity decrease at the UV branch of the deuterium lamp, the absorption spectrometer could be used only at $\lambda \gtrsim 230$ nm. The transmitted or emitted light, respectively, was analyzed by a Spex monochromator and was detected by a cooled photomultiplier (EMI 9844 QB bialkali).

The lifetime of the emission was measured with a Vidicon camera Sit 500 (B&M Corp.). This equipment was used also for the measurements of the absorption spectra of diluted solutions ($c_0 \lesssim 0.1$ M) at normal pressure in the temperature range 278 K $\leq T \leq$ 298 K, whereas the absorption spectra of concentrated aqueous solutions ($c_0 > 0.1$ M) with $\epsilon > 1000$ M^{-1} cm^{-1} have been recorded by an Uvikon spectrograph (Kontron Co.) with a microcell (d = 0.01 mm). For the measurements of the extinction of solutions at 293 K $\lesssim T \lesssim$ 333 K, a double-beam spectrograph (Shimadzu) was used.

Results

Absorption Spectra. Figure 2 shows the absorption spectrum of an aqueous solution ($c_0 = 10^{-4}$ M) of BaCP at T = 298 K and at p = 1 bar. The spectrum is composed of two strong bands, III and V, and two weak bands, II and IV. The low-energy part

(1) Gliemann, G.; Yersin, H. *Struct. Bond.* **1985**, *62*(87).
(2) Holzapfel, W.; Yersin, H.; Gliemann, G.; Otto, H. H. *Ber. Bunsenges. Phys. Chem.* **1978**, *82*, 207.
(3) Yersin, H.; Gliemann, G. *Ann. N. Y. Acad. Sci.* **1978**, *313*, 539.
(4) Tuszynski, W.; Gliemann, G. *Ber. Bunsenges. Phys. Chem.* **1985**, *89*, 940.
(5) Hidvegi, I.; v. Ammon, W.; Gliemann, G. *J. Chem. Phys.* **1982**, *76*, 4361. v. Ammon, W.; Hidvegi, I.; Gliemann, G. *Ibid.* **1984**, *80*, 2837.
(6) Gliemann, G. *Comments Inorg. Chem.* **1986**, *5*, 263.
(7) Yersin, H.; Hidvegi, I.; Gliemann, G.; Stock, M. *Phys. Rev.* **1979**, *B19*, 177.
(8) Dillinger, R.; Gliemann, G.; Pfleger, H. P.; Krogmann, K. *Inorg. Chem.* **1983**, *22*, 1366.
(9) Khvostikov, I. A. K. *Tr. Gos. Opt. Inst.* **1936**, *12*, 210.
(10) Ryskin, A. I.; Tkachuk, A. M.; Tolstoi, N. A. *Opt. Spectrosc. (Engl. Transl.)* **1964**, *17*, 304; **1964**, *17*, 390; **1966**, *21*, 31. Tkachuk, A. M.; Tolstoi, N. A. *Ibid.* **1966**, *20*, 570. Tolstoi, N. A.; Tkachuk, A. M. *Ibid.* **1966**, *21*, 310.
(11) Rossiello, L. A.; Furlani, C. *Lincei-Rend. Sc. Fis. Mat. Nat.* **1965**, *38*, 207.
(12) Webb, D. L.; Rossiello, L. A. *Inorg. Chem.* **1971**, *10*, 2213.
(13) Schindler, J. W.; Fukuda, R. C.; Adamson, A. W. *J. Am. Chem. Soc.* **1982**, *104*, 3596.
(14) Brauer, G. *Handbuch der präparativen anorganischen Chemie*; Georg Thieme Verlag: Stu'tgart, 1962; Vol. 2.
(15) Holzapfel, V . Thesis, Universität Regensburg, Regensburg, FRG, 1978.
(16) Mason, W. R.; Gray, H. B. *J. Am. Chem. Soc.* **1968**, *90*, 5721.
(17) Weis, C. E.; Piermarini, G. J.; Block, S. *Rev. Sci. Instrum.* **1969**, *40*, 1133; Barnett, J. P.; Block, S.; Piermarini, G. J. *Ibid.* **1973**, *44*, 1.
(18) Noak, R. A.; Holzapfel, W. B. *High-pressure Science and Technology*; Plenum Press: New York, 1979; Vol. 1.

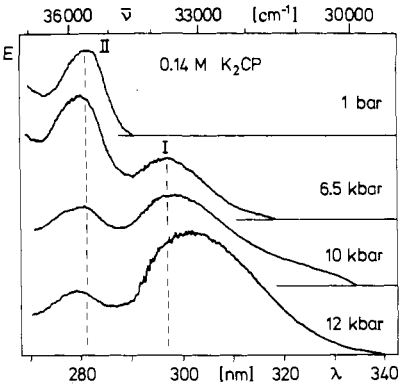

Figure 4. Absorption bands I and II of an aqueous solution of K_2CP at different pressures, p. c_0 = 0.14 M. T = 298 K.

Table I. Pressure-Induced Red Shift, $\Delta\bar{\nu}_I/\Delta p$, of Absorption Band I of Aqueous BaCP and K_2CP Solutions of Different Concentrations, c_0. T = 298 K

compd	c_0, M	$\Delta\bar{\nu}_I/\Delta p$, cm^{-1}/kbar
BaCP	0.05	−65 ± 20
	0.08	−60 ± 20
	0.10	−115 ± 20
K_2CP	0.10	−60 ± 20
	0.14	−150 ± 20

of the 298 K spectrum ($\lambda \gtrsim 230$ nm) has been studied at different pressures, p, for different concentrations, c_0, and for different cations of the tetracyanoplatinates(II). With increasing pressure, bands II, III, and IV are blue shifted, as shown for a BaCP solution (c_0 = 0.01 M) at T = 298 K in Figure 3. As an example, the energy of the maximum of band III versus pressure is plotted in the inset of Figure 3 for BaCP solutions with c_0 = 0.01 and 0.05 M, respectively. The slope $\Delta\bar{\nu}/\Delta p$ of band II is smaller by a factor of ~2.5 than that of band III. Variation of the cation and of the concentration does not change the slopes, $\Delta\bar{\nu}/\Delta p$, of bands II and III beyond the limits of reproducibility (±20%). The value of the slope, $\Delta\bar{\nu}/\Delta p$, of band IV could not be determined quantitatively because of the indistinct band shape.

The spectral positions of bands II–V depend also on the solvent, corresponding to the following order of the band maxima: $\bar{\nu}^{\alpha}$(in H_2O) > $\bar{\nu}^{\alpha}$(in C_2H_5OH) > $\bar{\nu}^{\alpha}$(in CH_3CN) ~ $\bar{\nu}^{\alpha}$(in CH_2Cl_2) ~ $\bar{\nu}^{\alpha}$(in $[CH_2Cl]_2$), with α = II, III, IV, or V. Thus, the absorption is blue shifted with increasing protic character of the solvent. A transition from the solvent CH_3CN to H_2O yields for bands II, III, and V blue shifts of about 400, 900, and 1300 cm^{-1}, respectively.

With increasing pressure, an additional band, I, grows up at the low-energy side of the absorption spectrum, as shown in Figure 4 for a 0.14 M K_2CP solution. In contrast to bands II, III, and IV, which exhibit a blue shift, band I is strongly red shifted with increasing pressure, as shown in Table I. The plots of the maximum extinction of band I versus pressure are shown in Figure 5 for different concentrations of BaCP and K_2CP in aqueous solutions. At low concentrations, the slopes of graphs $E = E(p)$ are linear over the whole pressure range 1 bar ≤ p ≲ 17 kbar; at higher concentrations, however, the extinction increases faster at $p \gtrsim 12$ kbar than at lower pressures. By extrapolation of the graphs to E = 0, the value of the lowest pressure, $\tilde{p}$, at which band I appears can be found. $\tilde{p}$ depends on the cation of the tetracyanoplatinate(II) and decreases with increasing concentration of the solution. For BaCP solutions with c_0 = 0.05 and 0.10 M, the $\tilde{p}$ values are 5 and 2.5 kbar, respectively.

As reported by Adamson et al.,[13] the absorption spectra of highly concentrated K_2CP solutions at p = 1 bar and T = 295 K show a weak band, I′, at $\lambda \sim 300$ nm. This band corresponds obviously to the pressure-induced band, I. The extinction of band I′ (at p = 1 bar) is proportional to the cube of the concentration, c_0, whereas band II follows Lambert–Beer's law. As we have found, the slope of the graph showing the extinction, E, of band

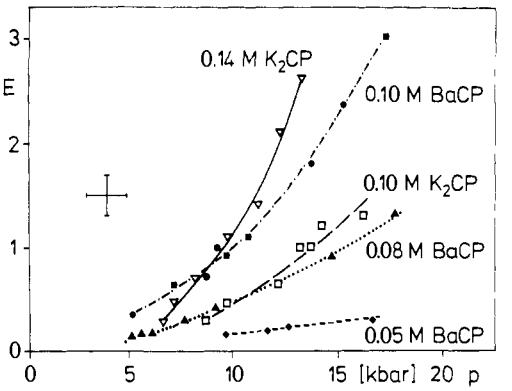

Figure 5. Maximum extinction, E, of band I of aqueous solutions of BaCP (c_0 = 0.05, 0.08, 0.10 M) and K_2CP (c_0 = 0.10, 0.14 M) as a function of pressure, p. T = 298 K. d = 0.1 mm.

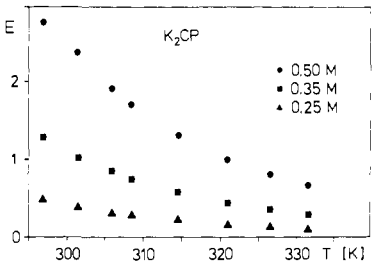

Figure 6. Extinction, E, of band I′ of aqueous solutions of K_2CP (c_0 = 0.25, 0.35, 0.50 M) at λ = 320 nm as a function of temperature, T. p = 1 bar. d = 1 mm.

I′ versus c_0^3 depends also on the cation; e.g., for Cs_2CP and K_2CP, the slope $\Delta E/\Delta(c_0^3\ M^{-3})$ has the values ~3.5 and ~2.5, respectively. The ratio of the maximum extinction values of bands I′ (at λ = 300 nm) and II (at λ = 280 nm), $E^{I'}{}_{300}/E^{II}{}_{280}$, also depends on the cation and on the concentration. For example, for solutions of Cs_2CP, K_2CP, and SrCP with c_0 = 0.3 M, this ratio has the value 0.25, 0.20, and 0.15, respectively. For highly concentrated solutions of $(n\text{-}Bu_4N)_2CP$ in dichloroethane, band I′ does not exist at all. The value of $E^{I'}{}_{300}/E^{II}{}_{280}$ for solutions of maximum concentration (e.g., $E^{I'}{}_{300}/E^{II}{}_{280} \sim 0.4$ for $c_0 \sim 0.7$ M SrCP) does not reach by far the value of $E^{I}{}_{300}/E^{II}{}_{280}$, which results for low-concentrated solutions by application of high pressure (e.g., $E^{I}{}_{300}/E^{II}{}_{280} \sim 2$ for 0.14 M K_2CP at p = 12 kbar, cf. Figure 4).

For low-concentrated solutions at p = 1 bar, band I′ can be lured out by lowering the temperature. For example, a 0.095 M K_2CP solution at T = 298 K does not exhibit band I′. At T = 278 K, however, this solution shows band I′ with $E^{I'}{}_{300}/E^{II}{}_{280}$ = 0.14. This value corresponds to a 0.24 M K_2CP solution at T = 298 K. On the other hand, a solution at T = 298 K, which absorbs at $\lambda \sim 300$ nm, reduces the extinction of band I′, if it is warmed up to T > 298 K, cf. Figure 6.

Emission Spectra. At ambient conditions (p = 1 bar and T = 298 K), aqueous solutions of tetracyanoplatinate(II) show an emission if the concentration, c_0, is not lower than 0.14 M and if the wavelength of the exciting light, λ_{exc}, is not longer than ~400 nm. The intensity of the emission augments with an increase of the concentration and with a decrease of the excitation wavelength. The maximum value of the wavelength, $\lambda_{exc}{}^{max}$, which just yields an emission, depends on the concentration, c_0. For example, K_2CP solutions of concentrations c_0 = 0.28 and 0.56 M can be excited by $\lambda \leq \lambda_{exc}{}^{max}$ = 360 and 400 nm, respectively.

Figure 7 shows the emission spectra of K_2CP solutions for different concentrations with λ_{exc} = 350 nm. The 0.56 M solution emits 10 times more intensively than the 0.28 M solution. With 0.56 M solution, the spectrum is composed of two bands, 1 and 3, and a weak shoulder, 2, whereas the 0.28 M solution exhibits only bands 1 and 3. The maxima of the bands denoted by 3 in both spectra have equal energies. Band 1 of the 0.56 M solution, however, is lower in energy by ~1000 cm^{-1} and has a smaller

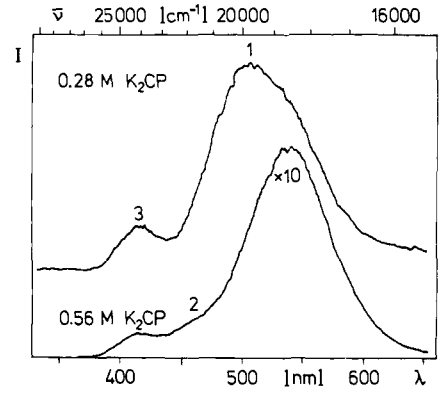

Figure 7. Emission spectra of aqueous solutions of K_2CP with $c_0 = 0.28$ and 0.56 M, respectively. $T = 298$ K. $p = 1$ bar. $\lambda_{exc} = 350$ nm. The symbol ×10 indicates that the intensity is 10 times higher than shown.

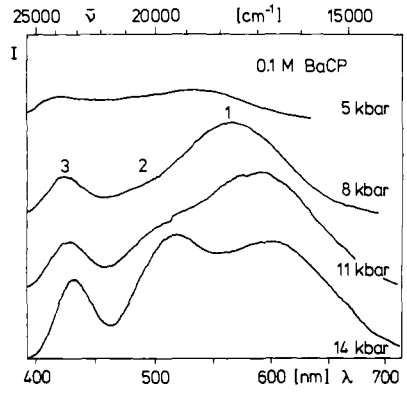

Figure 8. Emission spectrum of an aqueous solution of BaCP at different pressures, p. $c_0 = 0.1$ M. $T = 298$ K. $\lambda_{exc} = 364$ nm.

halfwidth than band 1 of the 0.28 M solution.

At ambient conditions and at an excitation wavelength $\lambda_{exc} = 364$ nm, a tetracyanoplatinate(II) solution shows no emission, if the concentration, c_0, is lower than 0.14 M. However, by application of a pressure $p \geq \tilde{p}$, which is high enough for the appearance of band I in the absorption spectrum, solutions of concentration $0.05\ \text{M} \leq c_0 \leq 0.14$ M emit, and the intensity of their emission increases with increasing pressure. Solutions with $c_0 < 0.05$ M show no emission up to $p = 15$ kbar.

The shape of the emission spectra depends distinctly on the value of the applied pressure. This pressure dependence varies both with the concentration of the solution and with the cation. A 0.1 M BaCP solution exhibits at $p = 3$ kbar only one weak emission band of type 3 ($\lambda_{max} \sim 420$ nm). An increase of pressure to $p \sim 5$ kbar gives rise to a nearly equally intense band of type 1 ($\lambda_{max} \sim 540$ nm), cf. Figure 8. With a further increase of pressure, the intensities, I_1 and I_3, of bands 1 and 3, respectively, grow, I_1 much more than I_3. At pressures $p \geq 11$ kbar, I_1 remains constant, whereas I_3 augments slightly with increasing pressure. At $p \sim 10$ kbar, an additional band 2 appears. Its intensity, I_2, reaches at $p \sim 14$ kbar a value comparable with that of I_1. A pressure increase shifts bands 3 and 1 to the red. For band 2, a Gaussian analysis of the spectra yields a red shift, which is slightly smaller than that of band 1.

The emission spectrum of a 0.08 M BaCP solution exhibits at $p \sim 6$ kbar only a weak band of type 3. With increasing pressure, two bands of type 1 and 2 appear and their intensities grow, but they do never exceed the intensity of band 3. At $p \sim 15$ kbar, the three bands have approximately equal heights.

A 0.10 M K_2CP solution shows a pressure dependence of its emission spectrum, which is very similar to that of a BaCP solution of equal concentration. A resembling behavior has been observed also with a 0.14 M K_2CP solution in the pressure range $p \lesssim 10$ kbar, cf. Figure 9. At higher pressures, however, there are pronounced differences. The intensity of band 3 decreases above 10 kbar. Band 2 reaches at $p \sim 12$ kbar its maximum intensity and decreases with further pressure increase.

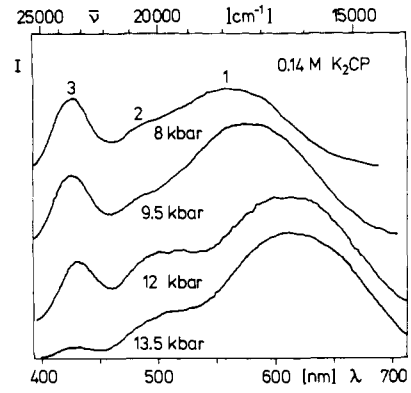

Figure 9. Emission spectrum of an aqueous solution of K_2CP at different pressures, p. $c_0 = 0.14$ M. $T = 298$ K. $\lambda_{exc} = 364$ nm.

Table II. Pressure-Induced Red Shifts, $\Delta\bar{\nu}/\Delta p$, of Emission Bands 1 and 3 of Aqueous BaCP and K_2CP Solutions of Different Concentrations, c_0[a]

compd	c_0, M	$\Delta\bar{\nu}/\Delta p$, cm⁻¹/kbar band 1	band 3
BaCP	0.08	−110	−65
	0.10	−220	−70
K_2CP	0.10	−120	−70
	0.14	−330	
	0.57	−250	

[a] $T = 298$ K. $\lambda_{exc} = 364$ nm. Because of its relatively low intensity, the red shift of band 3 could not be determined quantitatively for K_2CP solutions with $c_0 = 0.14$ and 0.57 M.

For a 0.57 M K_2CP solution at $p \sim 2$ kbar, only band 1 can be observed. With increasing the pressure, band 1 is red shifted without a change of its intensity. The intensity increase of band 2 is much smaller than for the 0.14 M K_2CP solution.

Table II shows the pressure-induced red shift, $\Delta\bar{\nu}/\Delta p$, of emission bands 1 and 3 for several BaCP and K_2CP solutions at room temperature.

Although at room temperature pure water crystallizes at pressures $p \gtrsim 10$ kbar,[19] no indication of the formation of ice could be found in all the high-pressure experiments with aqueous solutions of MCP reported above. The solutions were transparent and clear. By control experiments, it has been confirmed that these solutions were indeed in the liquid state. Upon cooling of MCP solutions at ambient pressure below 0 °C, the solutions lose their transparency, the light is scattered, and an absorption spectrum can no longer be measured. This indicates the formation of ice crystals, which were never observed in our high-pressure experiments. In other experiments with MCP solutions at room temperature, we have observed both the formation of a fine precipitate, which shows the emission properties of the corresponding solid MCP, as well as the disappearance of the extinction of the sample, if the pressure exceeds a certain value, which depends on the concentration of the solution (e.g., $p \sim 13$ kbar for 0.14 M K_2CP). The precipitate is obviously composed of small single crystals of MCP. The formation of such single crystals, however, is only possible if the sample is liquid.

Discussion

The absorption spectra of diluted solutions ($c_0 \lesssim 0.14$ M) at ambient conditions ($p = 1$ bar, $T = 298$ K) can be traced back to electronic transitions in the single complex ions $[Pt(CN)_4]^{2-}$.[1,20] Figures 10 and 11 show the corresponding energy level diagrams for the one-electron and the many-electron schemes, respectively. Band I′, which grows with increasing concentration, is due to the

(19) D'Ans Lax *Taschenbuch für Chemiker und Physiker*; Springer-Verlag: Berlin, 1972; Vol. I.
(20) Isci, H.; Mason, W. R. *Inorg. Chem.* **1975**, *14*, 905.
(21) Koster, H.; Franck, E. U. *Ber. Bunsenges. Phys. Chem.* **1969**, *73*, 716.
(22) Bridgman, P. W. *Proc. Am. Acad. Arts Sci.* **1941**, *74*, 419.

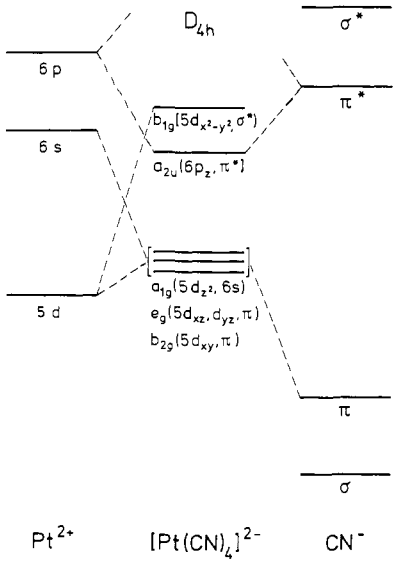

Figure 10. One-electron MO diagram of a single $[Pt(CN)_4]^{2-}$ ion (schematic diagram). Symmetry D_{4h}. The LUMO $a_{2u}(6p_z, \pi^*)$ is strongly stabilized by the interaction between $6p_z$(Pt) and $\pi^*(CN^-)$.

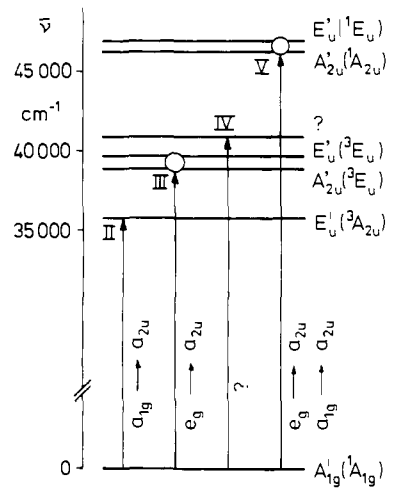

Figure 11. Assignment of absorption bands II–V to transitions between the many-electron states of a single $[Pt(CN)_4]^{2-}$ ion (schematic diagram).[20] Symmetry D_{4h}; spin-orbit coupling included.

formation of oligomers $[Pt(CN)_4]_n^{2n-}$ corresponding to the equilibrium relation

$$n[Pt(CN)_4]^{2-} \overset{K_{1n}}{\rightleftharpoons} [Pt(CN)_4]_n^{2n-} \qquad (1)$$

with $n = 3$.[13] This relation yields $c_n = c^n_M K_{1n}$ where c_n and c_M are the molar concentrations of the oligomer and the monomer, respectively. Using the spectral data in the range 290 nm $\leq \lambda \leq$ 325 nm, which are attached exclusively with band I′, one can derive from Beer's law, $E = \epsilon_n c_n d$, and from the concentration relation, $c_0 = c_M + c_n n$, the following formula

$$c_0 E^{-1/n} = \frac{n}{\epsilon_n d} E^{(n-1)/n} + [K_{1n}\epsilon_n d]^{-1/n} \qquad (2)$$

where E is the extinction, ϵ_n the molar extinction coefficient of the oligomer, c_0 the formality, and d the thickness of the sample. The graphs of $c_0 E^{-1/3}$ versus $E^{2/3}$ are straight lines with slope $3(\epsilon_3 d)^{-1}$ and intersect the ordinate at $(K_{13}\epsilon_3 d)^{-1/3}$, indicating the presence of trimers ($n = 3$). Since d is known, the molar extinction, ϵ_3, and the equilibrium constant, K_{13}, can be determined. In Table III, data for solutions of K_2CP, Cs_2CP, and SrCP, as examples, are summarized. The K_{13} value for K_2CP is distinctly smaller than for Cs_2CP. This effect is probably due to a stronger hindrance of the formation of oligomers by the hydrated cation of the bigger size ($r^{K^+}_{hydr} > r^{Cs^+}_{hydr}$).

Table III. K_{13} Values (Monomer–Trimer Equilibrium) and Extinction Coefficients, ϵ_3, of the Trimers at λ = 295 nm for Aqueous Solutions of K_2CP, Cs_2CP, and SrCP[a]

compd (concn range, M)	K_{13}, M^{-2}	ϵ_3, M^{-1} cm^{-1}
K_2CP ($0.16 \leq c_0 \leq 0.47$)	0.7	6000
Cs_2CP ($0.26 \leq c_0 \leq 0.38$)	1.4	4500
SrCP ($0.32 \leq c_0 \leq 0.70$)	0.5	4500

[a] T = 298 K. p = 1 bar. For K_2CP, the value of ϵ_3 decreases to ~1000 M^{-1} cm^{-1} if λ is increased to ~315 nm.

Table IV. K_{13} Values (Monomer–Trimer Equilibrium) and Values of the Wavelength, λ_{max}, of the Maximum of Absorption Band I of Aqueous BaCP and K_2CP Solutions at Different High Pressures, p. T = 298 K

	K_{13}, M^{-2}		
p, kbar	BaCP	K_2CP	λ_{max}, nm
7	4 ± 1	1.5 ± 1	~302
8	5.5	4.5	~303
9	6.5	7.5	~304
9.5	8.0	9.5	~304

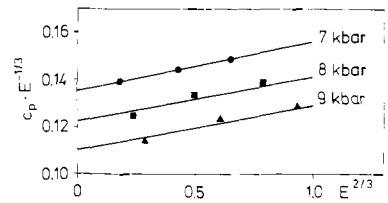

Figure 12. Plots of $c_p E_{max}^{-1/3}$ versus $E_{max}^{2/3}$ corresponding to eq 2 with n = 3 at p = 7, 8, and 9 kbar. c_p is the concentration at pressure p, calculated from $c_p = c_0 F$ where $F(p)$ is the compressibility factor of water.[21,22]

By the procedure described above, the temperature dependence of K_{13} can be evaluated. For example, between T = 297 and 332 K, the K_{13} value for K_2CP solutions with 0.16 M $\leq c_0 \leq$ 0.47 M varies from K_{13} ~0.9 to ~0.2 M^{-2}, indicating a decomposition of the oligomers with increasing temperature.

The enthalpy, $\Delta H°$, and the entropy, $\Delta S°$, of the formation of oligomers (n = 3) from the monomers can be determined directly from spectroscopical data using the relations

$$\ln K_{13} = -\frac{\Delta H°}{RT} + \frac{\Delta S°}{R} \qquad (3)$$

$$\ln E = -\frac{\Delta H°}{RT} + \frac{\Delta S°}{R} + \ln (\epsilon_n c^n_M d) \qquad (4)$$

For K_2CP solutions, the plots of ln $E(\lambda)$ versus $1/T$ are straight lines, yielding $\Delta H° \sim -35$ kJ/mol. With eq 3, the entropy value $\Delta S° \sim -122$ J/(K·mol) results. Variations of the concentration and of the wavenumber in the ranges 0.2 M $\lesssim c_0 \lesssim$ 0.4 M and 315 nm $\leq \lambda \leq$ 320 nm, respectively, do not change these values within the limits of experimental error.

As described above, diluted solutions of tetracyanoplatinates(II) with $c_0 <$ 0.14 M, which do not absorb in the spectral range of band I′ at p = 1 bar, exhibit an absorption band, I, at high pressures ($p \geq \tilde{p}$). It is a reasonable assumption that this band also is due to oligomers $[Pt(CN)_4]_n^{2n-}$. By the use of eq 2, the analysis of the spectral data yields for n the value 3, cf. Figure 12. Values of the equilibrium constant K_{13} for solutions of BaCP and K_2CP at different pressures are summarized in Table IV. By the application of a pressure of ~10 kbar, the value of K_{13} increases by a factor of ~10, indicating a distinct reduction of the volume, if a solution of monomers is transferred to a solution of oligomers.

The results reflect the difference of the two methods to change the concentration. By adding solute, the mole fraction and, thus, the probability of finding neighboring solute molecules are changed. By compression of the solution, the mole fraction is constant and the change in the concentration of the oligomer is

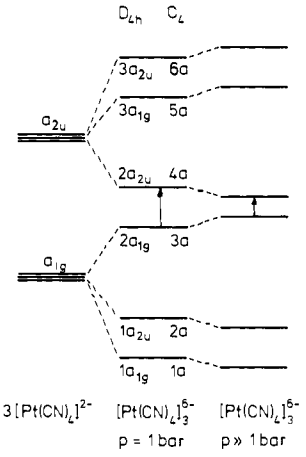

Figure 13. One-electron MO diagram of the HOMO's and LUMO's of single $[Pt(CN)_4]^{2-}$ ions (left-hand side), of a trimer $[Pt(CN)_4]_3^{6-}$ at p = 1 bar (middle part), and of a trimer at $p \gg 1$ bar (right-hand side), schematic diagram. The vertical arrows indicate the respective transitions of lowest energy.

predominantly due to a change of the equilibrium constant via a decrease in the partial molar volume on forming an oligomer.

In the trimers, the three $[Pt(CN)_4]^{2-}$ ions are expected to be stacked correspondingly to the columnar structure of the single crystalline tetracyanoplatinates(II).[1] If the three complex ions are arranged with face-to-face configuration or if neighboring complexes are mutually rotated by 45° around the stacking axis, the trimer has D_{4h} symmetry. Otherwise the symmetry is C_4. For a single-ion $[Pt(CN)_4]^{2-}$ and for the trimer $[Pt(CN)_4]_3^{6-}$, the one-electron energy levels of the highest occupied MO's and the lowest unoccupied MO's are shown schematically in Figure 13. Absorption band I′ (and I) can be assigned to the allowed singlet–singlet transition $a_{1g} \rightarrow a_{2u}$ (D_{4h}) or a → a (C_4). As indicated in Figure 13, the energy splitting of the states as well of a_{1g} parentage and of a_{2u} parentage increases with increasing pressure as a consequence of the reduction of the intratrimer Pt–Pt distance. Thus, the energy gap between the HOMO and the LUMO of the trimer becomes smaller, and band I is shifted to the red, as observed in the experiments, cf. Figure 4 and Table I.

With increasing concentration of aqueous solutions of tetracyanoplatinates(II) at ambient conditions, the absorption spectrum shows one additional band (I′), which could be traced back to trimers. The emission spectrum, however, exhibits three bands (1, 2, and 3). As shown by Adamson et al.,[13] these emission bands have been assigned to oligomers with $n > 5$, $n = 5$, and $n = 4$, respectively. The oligomers with $n \geq 4$ are assumed to be composed of n nearly equidistant $[Pt(CN)_4]^{2-}$ ions arranged with face-to-face configuration forming a column. They can be regarded as fragments of a chain of $[Pt(CN)_4]^{2-}$ ions of single-crystal tetracyanoplatinate(II).[1] A further emission band, 4 (at $\lambda \sim 350$ nm), can be observed if the solution is excited with $\lambda_{exc} = 313$ nm. Since at this wavelength the trimer absorbs, band 4 has been attributed to the emission of trimers. Band 1 is red shifted if the concentration of the solution is augmented. This effect can be explained by an increase of the mean length of oligomers with $n > 5$ and, thus, by a reduction of the mean value of the corresponding HOMO–LUMO gaps.

As shown above, tetracyanoplatinate(II) solutions of low concentration ($0.05 \text{ M} \lesssim c_0 < 0.14$ M) exhibit an emission, if high pressure ($p \gg 1$ bar) is applied to the solution. This effect indicates a pressure-induced formation of oligomers. At relatively low pressures, mainly band 3, which corresponds to tetramers, has developed. (In our experiment, trimer band 4 could not be observed, since an excitation wavelength $\lambda_{exc} = 364$ nm has been used. The absorption wavelength of the trimers, however, is $\lambda \sim 300$ nm.) With increasing pressure, in addition to band 3 the emission of pentamers (band 2) and polymers with $n > 5$ (band 1) occurs. Since the intensities of bands 1 and 2 rise more strongly than that of band 3, it can be concluded that the oligomers with $n \geq 5$ increase in number larger than the tetramers. In the concentration range $0.05 \text{ M} \lesssim c_0 < 0.14$ M, obviously the formation of pentamers is preferred, whereas at $c_0 \approx 0.14$ M polymers with $n > 5$ are favored.

The total emission of tetracyanoplatinate(II) solutions exhibits a pressure-induced red shift, which is similar to that of absorption band I. As shown in Table II, the pressure-induced red shift of band 3 is independent of the concentration, c_0. This fact confirms the above conclusion that only one kind of oligomer ($n = 4$) gives rise to band 3. The red shift of band 3 (and band 2) can be traced back to an increase of the intraoligomer Pt–Pt coupling due to a reduction of the intercomplex distance. Thus, the gap between the HOMO and the LUMO of the tetramer (and pentamer) decreases, cf. Figure 13.

On the other hand, band 1 exhibits a pressure-induced red shift that depends on the concentration, c_0. At $c_0 \lesssim 0.14$ M, the pressure-induced red shift is growing with increasing concentration. This indicates that in this concentration range, both by pressure increases and by concentration increases, additional oligomers of large size ($n \gg 5$) are formed. The observed broadening of band 1 with increasing pressure also is compatible with this explanation. At high concentrations ($c_0 > 0.4$ M), the $n \gg 5$ oligomers with nearly equal HOMO–LUMO distances are dominating. Then, the pressure-induced red shift is only due to the reduction of the gap between the HOMO and the LUMO of the $n \gg 5$ oligomers and will not be changed by a variation of the concentration. As an example, the red shift $\Delta\bar{\nu}/\Delta p = -250$ cm^{-1}/kbar of a 0.57 M K_2CP solution corresponds mainly to the reduction of the gap, whereas the larger red shift of -330 cm^{-1} found at $c_0 = 0.14$ M is composed of two effects, the reduction of the gap and the increase of the mean length of the oligomers with $n > 5$. That the half-width of band 1 is independent of c_0 at high concentrations confirms the proposed model.

The shape of band 1 at high concentrations resembles the $\mathbf{E} \perp \mathbf{c}$ emission band of single-crystal tetracyanoplatinates(II) at T = 298 K and p = 1 bar.[1] The emission decay times of both bands also are very similar ($\tau \sim 500$ ns). These facts suggest that we assign the oligomer band 1 to the spin-forbidden transition $E'_u(^3A_{2u}) \rightarrow A'_{1g}(^1A_{1g})$ at symmetry D_{4h}. For single-crystal tetracyanoplatinates(II), an empirical relation between the wavenumber, $\bar{\nu}_e$, of the $\mathbf{E} \perp \mathbf{c}$ emission maximum and the Pt–Pt distance R has been established,

$$\bar{\nu}_e(E'_u \rightarrow A_{1g}) = 36800 - 6.3 \times 10^5 R^{-3} \qquad (5)$$

with $\bar{\nu}_e$ and R in units of cm^{-1} and Å, respectively. Application of this relation to the "long" oligomers with $\lambda = 538$ nm (maximum of band 1 at p = 1 bar) yields a Pt–Pt distance of $R = 3.26$ Å in the oligomers. Similar values ($R = 3.25$ Å) have been found in single-crystal $KNa[Pt(CN)_4]\cdot 3H_2O$ and $Sr[Pt(CN)_4]\cdot 2H_2O$.[23]

For the linear compressibility, κ_c, parallel to the columns in single-crystal tetracyanoplatinates(II), the following relation holds, if eq 5 is used:

$$\kappa_c = -\frac{1}{R}\frac{\Delta R}{\Delta p} = -\frac{R^3}{3 \times 6.3 \times 10^5}\frac{\Delta\bar{\nu}_e}{\Delta p}$$

With $\Delta\bar{\nu}/\Delta p = -250$ cm^{-1}·kbar^{-1} for the "long" oligomers, this relation yields $\kappa_c = 4.5 \times 10^{-3}$ kbar^{-1}, which is very similar to the values found for single-crystal $Na_2CP\cdot 3H_2O$, $BaCP\cdot 4H_2O$, and $MgCP\cdot 7H_2O$.[1]

For the pressure-induced blue shift of absorption bands II–V, which belong to the monomer, we have no obvious and plain interpretation, and we are rather obliged to speculate upon the reason of this effect. A reduction of the intracomplex Pt–CN distance by the application of high pressure as a reason for the blue shift can be ruled out. As Figure 10 shows, such a reduction would yield an increase of the metal–ligand overlap, resulting in an energy increase of the HOMO and a lowering of the LUMO energy, and thus, a red shift but not a blue shift is expected.

(23) Holzapfel, W.; Yersin, H.; Gliemann, G. *Z. Kristallogr.* **1981**, *157*, 47.

However, it is possible that hydrogen bonding between the solvent molecules H_2O and the nitrogen atoms of the CN ligands is effective. This bonding reduces the density of the π-electrons in the neighborhood of the central ion, and the overlap becomes weaker. Thus, the energy gap between the HOMO and the LUMO is enlarged. With increasing pressure, this effect will be strengthened, and as a consequence, absorption bands II–V are shifted to higher energies. That bands III and V show distinctly larger blue shifts than band II can be traced back to the different symmetries of the MO's from which the corresponding excitations start. Whereas the HOMO of bands III and V, $e_g(5d_{xy}, d_{yz}, \pi)$, contains a π-component due to the metal–ligand overlap, the HOMO of band II, $a_{1g}(5d_{z^2})$, is a pure metal state. This speculative model is supported by the above-mentioned dependence of the absorption energies on the solvent, where, with increasing protic character of the solvent, bands II–V are blue shifted.

Acknowledgment. This research has been supported by the Deutsche Forschungsgemeinschaft and the Fonds der Chemischen Industrie.

Metallacarboranes in Catalysis. 8. I: Catalytic Hydrogenolysis of Alkenyl Acetates. II: Catalytic Alkene Isomerization and Hydrogenation Revisited

James A. Belmont, Jorge Soto, Roswell E. King, III, Andrew J. Donaldson, John D. Hewes, and M. Frederick Hawthorne*

Contribution from the Department of Chemistry and Biochemistry, The University of California at Los Angeles, Los Angeles, California 90024. *Received October 31, 1988*

Abstract: Part I of this study describes the facile hydrogenolysis (and deuteriolysis) of alkenyl acetates, such as isopropenyl acetate (D) and 1-phenylvinyl acetate (E), with rhodacarborane catalyst precursors to yield acetic acid and the corresponding alkene. The catalyst precursors employed were [*closo*-3,3-$(PPh_3)_2$-3-H-3,1,2-$RhC_2B_9H_{11}$] (I), [*closo*-2,2-$(PPh_3)_2$-2-H-2,1,7-$RhC_2B_9H_{11}$] (II), and [*closo*-2,2-$(PPh_3)_2$-2-H-2,1,12-$RhC_2B_9H_{11}$] (III). The hydrogenolysis of alkenyl acetates D and E produced propene and styrene, respectively, along with acetic acid in essentially quantitative yields. Deuterium at Rh was demonstrated not to enter the hydrogenolysis reaction. Use of D_2 as the reducing agent with I and E resulted in the incorporation of deuterium into reactant E and products. Styrene produced in these reactions was predominantly d_1 with appreciable quantities of d_0 and d_2. Ethylbenzene, a byproduct resulting from the hydrogenation of styrene, contained only traces of d_0 species and was largely d_1, d_2, and d_3. The acetic acid formed in these reactions was isotopically pure CH_3COOD. The rate law for E hydrogenolysis with I contained no term showing hydrogen dependence. These results suggest a reaction mechanism for hydrogenolysis that is based upon the relatively slow formation and decomposition of a very reactive rhodium(III) monohydride formed through the regioselective oxidative addition of Rh^I (in the exo-nido tautomer of the rhodacarborane) to terminal B–H bonds. The monohydride produced in this fashion then enters a cyclic heterolysis process with H_2 which leads to rapid product formation. This mechanism suggests that slow B–D/C–H exchange should occur between I-d_9 (B–D at all vertices of I) and an isotopically normal alkane, such as 1-hexene (B), during alkene isomerization. Such exchange was observed and shown to be regioselective. This new information predicated part II of this study, which is devoted to a modification of previously advanced proposals for the mechanisms of alkene isomerization and hydrogenation with rhodacarborane precursors. The facile and regioselective exchange of B–H in [*exo-nido*-$(PPh_3)_2$Rh-μ-7,8-$(CH_2)_3$-7,8-$C_2B_9H_{11}$] (IV) with D_2 was examined and shown to be electrophilic in character and to apparently proceed through very reactive monohydride intermediates. These new data coupled with previously reported results allow the formulation of unified mechanisms for B–H/D_2 and B–H/C–D exchange, alkenyl acetate hydrogenolysis, alkene isomerization, and alkene hydrogenation based upon the key B–Rh^{III}–H species formed by the regioselective oxidative addition of terminal B–H bonds to Rh^I centers. Thus, the effective catalytic sites in all of these reactions appear to be an array of B–Rh^{III}–H centers formed reversibly from the Rh^I present in *exo-nido*-rhodacarborane tautomers which are, in turn, in equilibrium with their corresponding closo tautomers. In deuterium-labeling reactions, the marked difference in regiospecificity displayed by I in contrast to the sterically encumbered IV is shown to be in agreement with these new proposals.

The insertion of alkenes into metal hydride linkages and the microscopic reverse of this reaction (β-elimination) are ubiquitous throughout organometallic chemistry.[1] However, a variant of this set of reactions in which the alkene is an alkenyl acetate presents the possibility of observing another sort of β-elimination from the metal β-acetatoalkyl formed by insertion.[2] This reaction course results in the formation of metal acetate and the alkene derived from the alkenyl acetate by formal interchange of the acetate group with hydride. The actual fate of alkenyl acetates

Scheme I

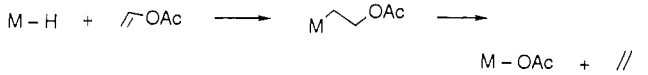

Scheme II

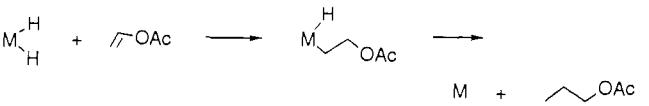

in the presence of metal hydrides has generally been determined by the number of available hydride ligands attached to the metal center. Thus, monohydrides provide stoichiometric cleavage of alkenyl acetate to metal acetate and alkene[2] (Scheme I), while dihydrides such as $H_2RhCl(PPh_3)_2$ can provide alkyl acetates via

(1) Collman, J. P.; Hegedus, L. S.; Norton, J. R.; Finke, R. G. *Principles and Applications of Organotransition Metal Chemistry*; University of Science Books: Mill Valley, CA, 1987.

(2) (a) Abatjoglow, A. G.; Bryant, D. R.; D'Esposito, L. C. *J. Mol. Catal.* **1983**, *18*, 381. (b) Komiya, J.; Yamamoto, A. *J. Organomet. Chem.* **1975**, *87*, 333.

0002-7863/89/1511-7475$01.50/0